

Final Report on

The Texas A&M University Project Entitled

“Rain maps Inferred from Polarimetric Radar Observations over Coastal Locales”

Submitted to

The University of Maryland Baltimore County (UMBC)

By

Dr. Lawrence D. Carey
Assistant Professor
Department of Atmospheric Sciences
Texas A&M University
College Station, Texas 77843-3150

On

February 28, 2007

Objectives:

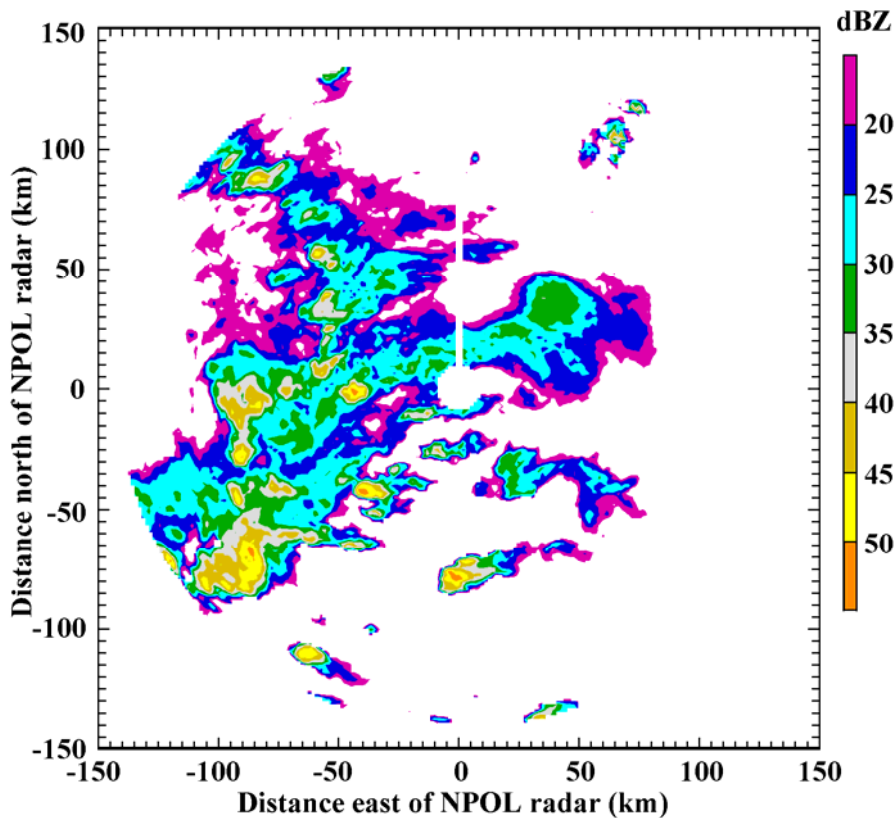
1. To assess the NPOL polarimetric performance relative to that of established polarimetric radars (e.g., CSU-CHILL, NCAR SPOL, and BMRC CPOL);
2. To evaluate the influence of “wet antenna” on the NPOL measurements.

Approaches:

The case of 25 June 2004 was selected to perform a detailed case study. One case from each other research radars, i.e., CSU-CHILL (16 July 2004), NCAR SPOL (26 January 1999 from TRMM-LBA, Cifelli et al. 2002), and BMRC CPOL (24 May 1998 from SCSMEX, Wang and Carey 2004), also in a widespread rain event was also studied for the comparison purpose.¹

1. Case Overview

On 25 June 2004, under the influence of a cold front passage, a set of convective rainbands passed the mid-Atlantic coast and caused widespread rainfall in the region. At the NPOL radar site, rain gauge data showed that a total of 8 mm rainfall was recorded from 1849 to 2050 UTC. The operation of the NPOL radar was from 1613 to 2330 UTC with continuous 6-min 360° surveillance scans at 10 elevations from 0.5° to 20°. Meanwhile, the SPANDAR radar was operated from 1700 to 2000 UTC with continuous 18-min 360° surveillance scans.



¹ With collaborative input from Dr. Jian-Jian Wang, UMBC GEST and NASA GSFC.

Fig. 1 NPOL radar reflectivity (dBZ) at 3 km MSL valid at 1843 UTC, 25 June 2004.

The rainband moved into the NPOL observational domain at 1615 UTC. The eastward propagating rainband enhanced in both size and intensity during the next 2.5 hours. At 1843 UTC, the main feature in the domain was the north-south-oriented frontal rainband with a width of 70-100 km (Fig. 1). This rainband has a maximum reflectivity of 58 dBZ recorded at 2125 UTC to the south of NPOL. The whole system weakened and moved out of the radar domain around 2330 UTC.

2. Estimation of the measurement bias

The original NPOL data was quality controlled by using the empirical method described by Carey et al. (2000). Light thresholding of range gate data of $\rho_{HV} \geq 0.6$ and $\sigma(\Psi_{dp}) \leq 18^\circ$ was used to remove clear air, clutter and other non-precipitation echo. The quality controlled radar data were then interpolated to a Cartesian grid using the National Center for Atmospheric Research (NCAR) SPRINT software (Mohr et al. 1986) for further analysis.

First, we estimated any possible Zdr bias by examining the histogram of Zdr in anvil echo. Using raw UF data, we isolated range gates characterized by low-to-moderate reflectivity (15-25 dBZ) at high elevation angle (≥ 15 deg) well above the bright band (> 6.0 km) at moderate ranges ($10 \leq \text{Range} \leq 60$ km). The goal is to isolate dry, low density aggregates which should have near zero Zdr. We found that Zdr had a positive bias of +0.46 dB. Strangely, there was a periodic behavior in the frequency histogram. After every one or two high frequency samples, there was a low frequency sample about half of the value from the trend of the previous two points. This may suggest a data digitization problem. Zdr should be accurate to 0.1 dB for quantitative use. Given this odd frequency histogram, we would suggest that NPOL has a potential problem, possibly with the way the data were recorded.

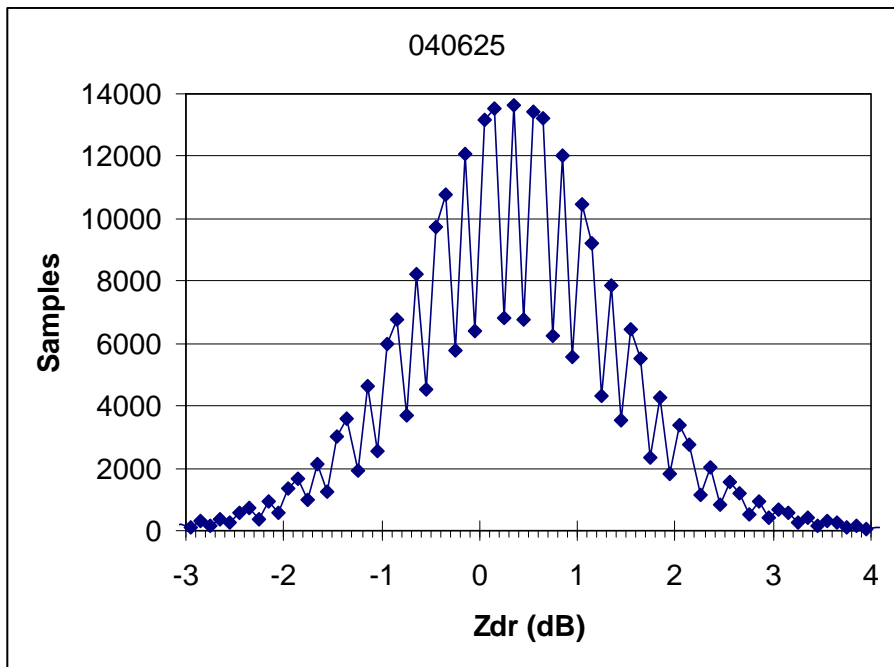


Fig. 2 Z_{DR} histograms from NPOL at 1843 UTC, 25 June 2004. Bin size is 0.1 dB.

We next compared the NPOL reflectivity data with Wakefield NEXRAD radar and Wallop S-band SPANDAR radar, which are 102 km southwest and 82 km northeast to the NPOL, respectively. With different radar characteristics, start and end time of the volumes from each radar, we should not expect “point-to-point” match of the data. As shown in Fig. 3, the slope of the linear interpolation for two S-band radars, NPOL and SPANDAR, in general was close to the perfect correlation (1:1) line. The NPOL reflectivity data are slightly, about 0.7 dBZ, higher than the SPANDAR reflectivity data. The correlation between NPOL and NEXRAD was about equally good. However, the NPOL had reflectivities about 1.7 dBZ higher than NEXRAD.

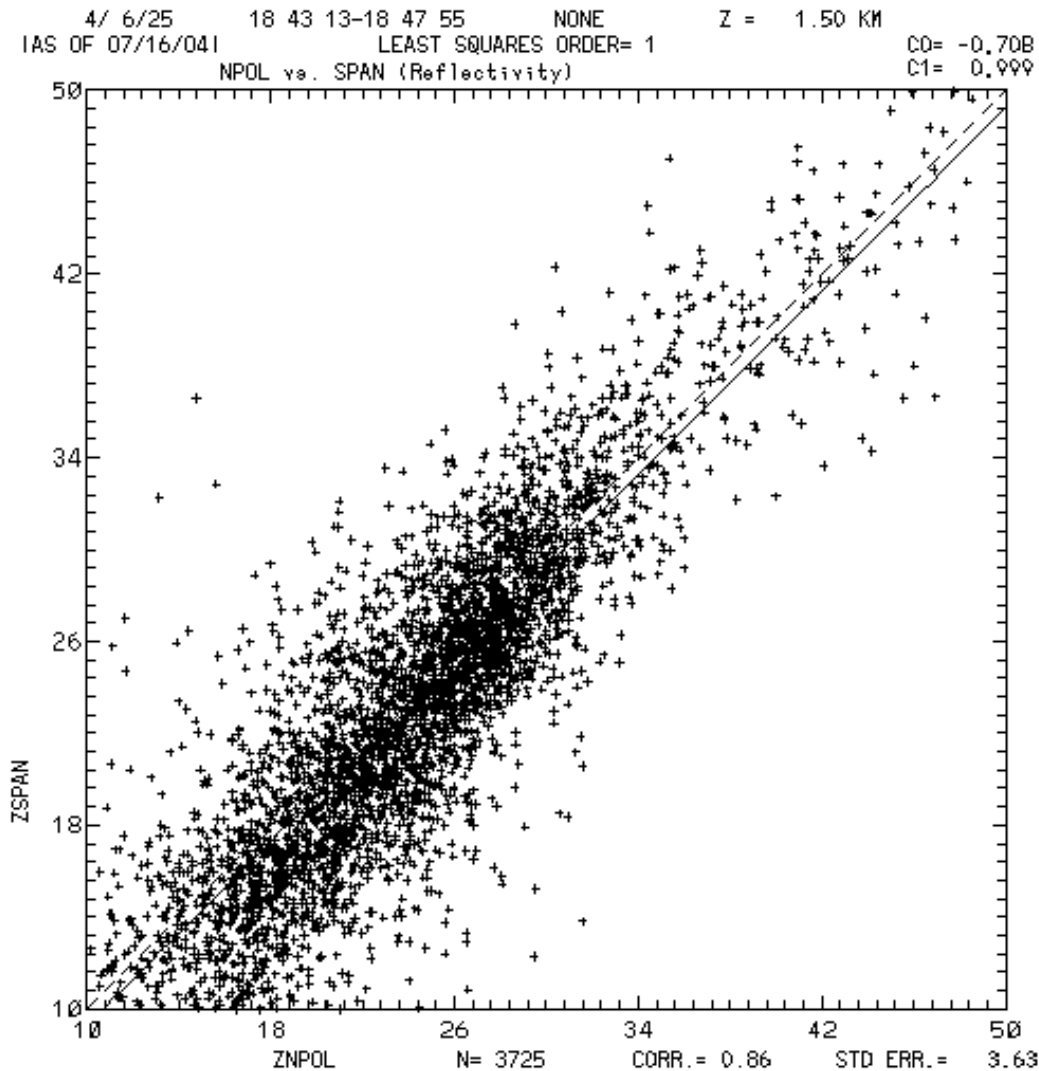


Fig. 3 Radar reflectivity comparison between NPOL and Wakefield NEXRAD at 1843 UTC, 25 June 2004.

3. Empirical Investigation of Relative Polarimetric Radar Performance

To compare NPOL with other established polarimetric radars, we took samples from 0.5 to 1.0 km AGL (well below melting level and above remaining clutter) and then restricted samples to a reflectivity range that is representative of drizzle and yet is less prone to low SNR and edge/high Zh gradient effects (e.g., $20 \leq Z_h \leq 25$ dBZ). Drizzle should be characterized approximately by $K_{dp} \approx 0^\circ \text{ km}^{-1}$, $Z_{dr} \approx 0$ dB, and $\rho_{HV} \approx 0.99$. In this data sample of “drizzle”, ρ_{HV} is a general indicator of data quality. Significant deviation (e.g., > 0.01) of ρ_{HV} below 0.99 in drizzle is an indication of general radar system (e.g., transmitter through receiver chain hardware or signal processing) issues. In drizzle, the standard deviation of the measured differential phase, $\sigma(\Psi_{dp})$, should afford an empirical approximation of differential phase measurement error. The $\sigma(\Psi_{dp})$ was estimated over the same number of range gates used to estimate K_{dp} (i.e., 21 gates). In the literature (e.g., see Doviak and Zrnica 1993; Bringi and Chandrasekar 2001 for review), a reasonable range of $\sigma(\Psi_{dp})$ is about 2° to 3° or lower for K_{dp} applications involving quality control, rain rate, drop size distribution, and hydrometeor identification. In drizzle, the absolute average deviation of Z_{dr} from its mean should provide an upper-end estimate of the random measurement error in Z_{dr} . For polarimetric applications, it is assumed that the random measurement error in Z_{dr} is a few tenths of a dB or less (e.g., approaching 0.2 dB is ideal and < 0.5 dB is required). Because of the limitations in isolating true “drizzle” in this fashion, it is expected that this approach will slightly overestimate the actual random measurement error in Z_{dr} (e.g., minor contribution, such as 0.1-0.2 dB, associated with physical variability in DSD and hence Z_{dr} may still be present).

Table 1. Polarimetric Radar Characteristics in “Drizzle” for Four Research Radars

RADAR	Date/Time (Z) YYMMDDHHMM	Number Gates (N)	Median Z_h	Median K_{dp}	Median ρ_{HV}	Median $\sigma(\Psi_{dp})^*$	AAD** Z_{dr}
CHILL	0407162142	4946	22.6 dBZ	$0.0^\circ \text{ km}^{-1}$	0.99	2.5°	0.4 dB
CPOL	9805242040	2416	22.6 dBZ	$0.0^\circ \text{ km}^{-1}$	0.99	2.3°	0.3 dB
NPOL	0406252131	4577	22.4 dBZ	$0.0^\circ \text{ km}^{-1}$	0.95	7.1°	0.9 dB
SPOL	9901262139	6827	22.5 dBZ	$0.0^\circ \text{ km}^{-1}$	0.99	1.4°	0.3 dB

* The standard deviation of the measured differential phase was computed at each range gate from a running, centered 21-gate sample. The value shown here is the median value from all range gates in the sample.

** $AAD Z_{dr} = \text{Average Absolute Deviation } Z_{dr} = \frac{1}{N} \sum_{i=1}^N |Z_{DR}(i) - \bar{Z}_{DR}|$

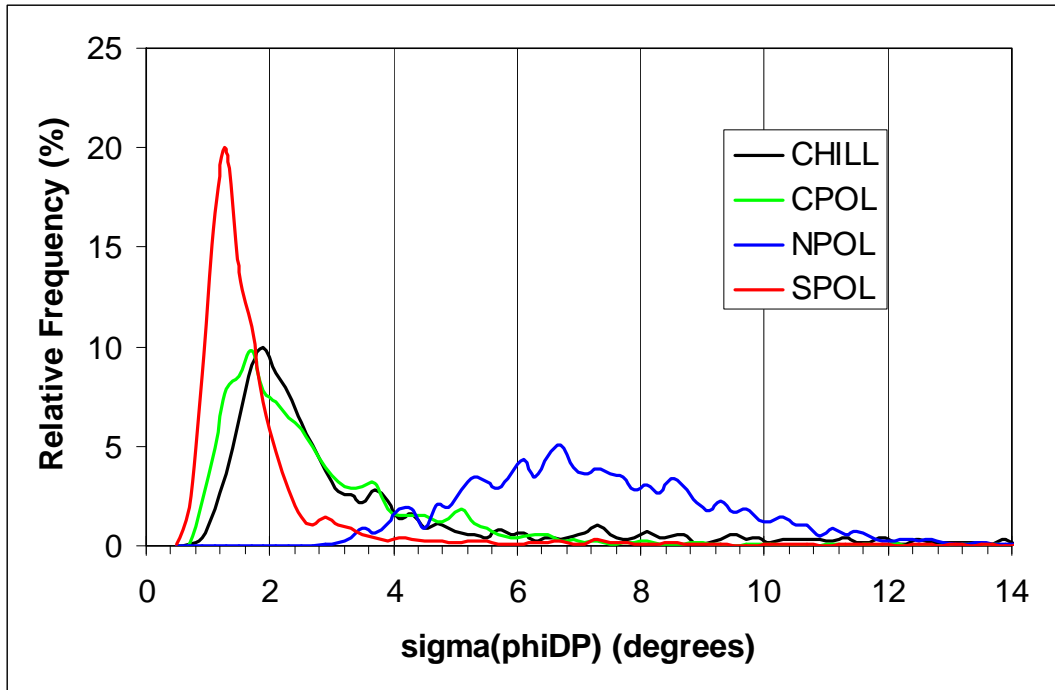


Fig. 4. Relative frequency histogram of the standard deviation of the measured differential phase (taken over running 21 gate sample) in “drizzle.”

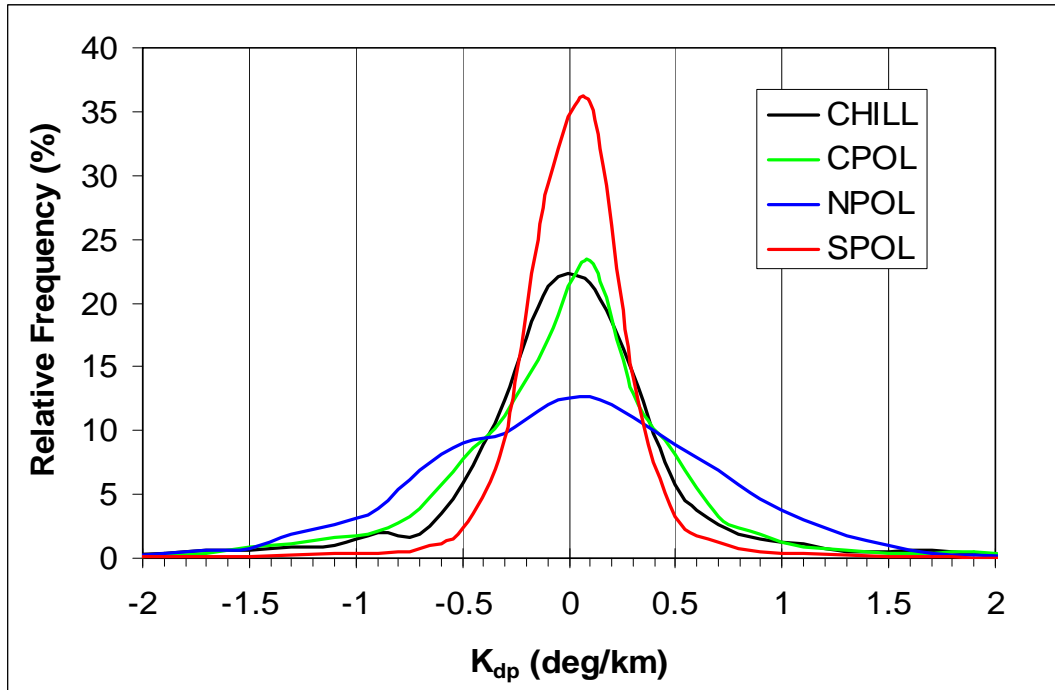


Fig. 5. Relative frequency histogram of the estimated specific differential phase in “drizzle.”

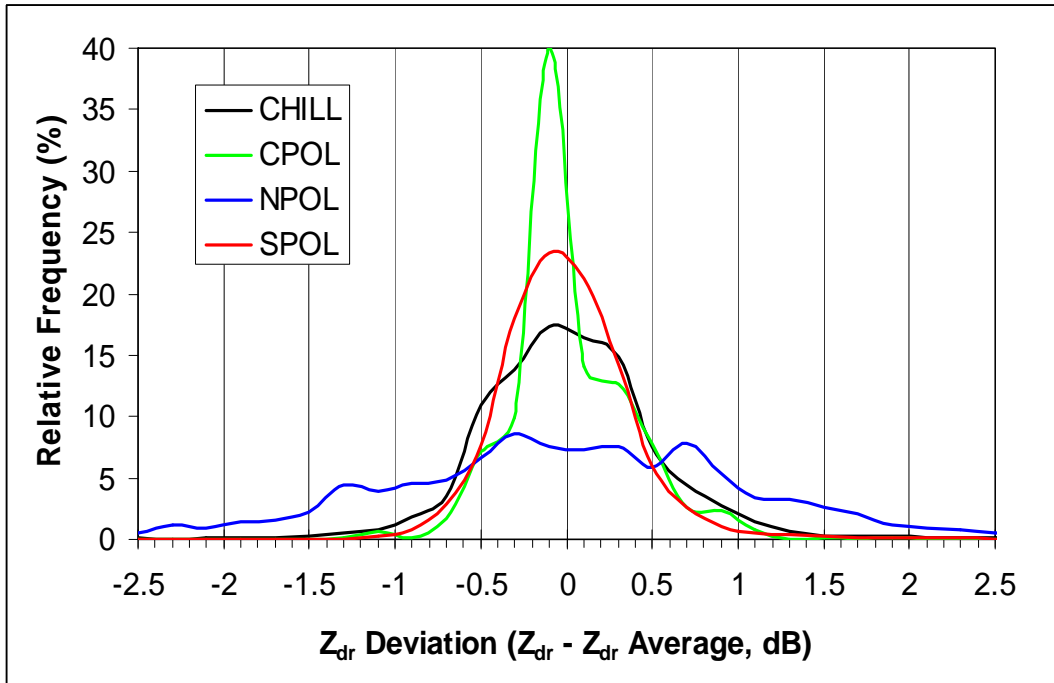


Fig. 6 Relative frequency histogram of the deviation of the differential reflectivity from its average (i.e., $Z_{DR}(i) - \bar{Z}_{DR}$) in “drizzle.”

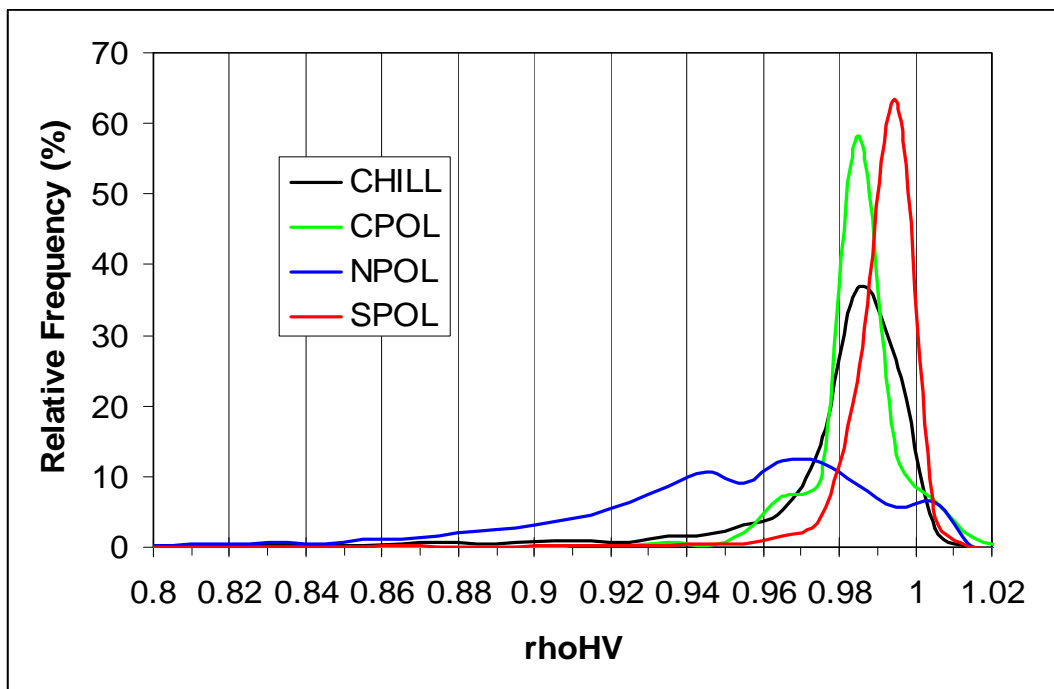


Fig. 7. Relative frequency histogram of the correlation coefficient between horizontal and vertical polarization signals in “drizzle.”

The results in Table 1 and Figures 4-7 demonstrate that polarimetric data quality for the relatively new NPOL radar is not yet up to the standards of other established research polarimetric radars in the international community (e.g., CSU-CHILL, NCAR SPOL, and BMRC CPOL). For example, the random measurement error in the measured differential phase is 3 to 5 times larger for NPOL than for the other established research radars (Table 1). More specifically, the measurement error in the NPOL differential phase (Ψ_{dp}) is about 7° compared to more typical values of 1.4° to 2.5° for the other radars (Figure 4). Because of the increased phase noise, the estimated specific differential phase (Kdp) is significantly more noisy (Figure 2). In drizzle, Kdp should be zero. Any deviation from zero is associated with measurement error. The NPOL Kdp distribution in drizzle is relatively flat with a significant fraction of $|Kdp|$ even beyond 1° km^{-1} . The distributions of Kdp for the other radars are much more peaked around zero. Similarly, the random measurement error in the differential reflectivity (Zdr) is 2 to 3 times larger for NPOL. In particular, an upper-end empirical estimate of the standard error in Zdr is 0.9 dB compared to about 0.3-0.4 dB for the other radars (Table 1). The deviation of Zdr from its average value in drizzle should be about zero. Notice how the distributions of Zdr are highly peaked about zero for the CPOL, SPOL, and CHILL radars while the NPOL Zdr distribution is very flat with significant contributions for $|Zdr| > 0.5 \text{ dB}$ (Figure 6).

These NPOL measurement errors above are consistent with generally depressed values of the NPOL correlation coefficient (ρ_{HV}) in the “drizzle” data (Table 1 and Figure 7). In polarimetric radar applications, ρ_{HV} is a measure of the correlation between horizontally and vertically polarized weather signals. It is most affected by the variability in the ratio of the vertical-to-horizontal physical size (i.e., shape) of hydrometeors in the radar resolution volume but it is also affected by variability in the hydrometeor canting angle (i.e., particle oscillations or wobbling), dielectric (i.e., ice vs. water fraction), and Mie scattering. Drizzle is nearly spherical and there is little or no variability in shape, canting angle, dielectric or Mie scattering within a radar resolution volume. As a result, the correlation coefficient between horizontally and vertically polarized weather signals in drizzle is theoretically near unity (≥ 0.99). Notice how the distribution of ρ_{HV} is very peaked around 0.99 and has little or no tail to lower values for the SPOL, CPOL and CHILL radar samples of drizzle (Figure 4). However, the measured correlation coefficient for a given hydrometeor type can be slightly different depending on the radar system’s performance (i.e., similar to Doppler spectrum width) and polarimetric purity. The latter can be decreased by several factors, including the degree of matching between the antenna patterns at H and V polarizations and the degree of isolation between H and V polarizations in the antenna and microwave assembly system (i.e., amount of cross-coupling between the two orthogonal channels in the entire transmitter-to-receiver chain). As the quality of the radar system decreases, the measured correlation coefficient decreases for a given hydrometeor type. For example, notice how the distribution of NPOL’s ρ_{HV} in drizzle is relatively flat with a broad peak from 0.94 to 0.98 and a long tail to values below 0.9 (Figure 4).

One can parameterize radar performance (such as error in the differential phase or differential reflectivity) as a function of the correlation coefficient (e.g., see Doviak and Zrnich, 1993 or Bringi and Chandrasekar, 2001, Sec. 6.5). In other words, one could have anticipated the increased noise in Ψ_{dp} (and hence Kdp) and Zdr based on the depressed values of ρ_{HV} alone. A decrease of median ρ_{HV} from 0.99 to 0.95 in drizzle is significant and

represents a serious increase in measurement error. All else being equal, this decrease in ρ_{HV} can account for the 2 to 5 times increase in the standard error in the NPOL differential phase and differential reflectivity compared to the other radars (Bringi and Chandrasekar, 2001, Sec. 6.5).

The implications of these errors are significant. Along with reflectivity, Zdr and Kdp are key parameters for the estimation of rain rate and other DSD parameters and the identification of hydrometeor types. The Zdr and especially the differential phase are also very important for data processing and quality control (e.g., power calibration, attenuation correction, and the removal of clutter, clear air and anomalous propagation). An increase in the measurement errors of these polarimetric radar parameters directly amplifies the error in the estimated rain rate or other DSD parameters (e.g., Chapter 8 of Bringi and Chandrasekar 2001). These measurement errors also decrease the effectiveness of algorithms for hydrometeor identification and data processing and quality control.

4. “Wet Antenna” Problem

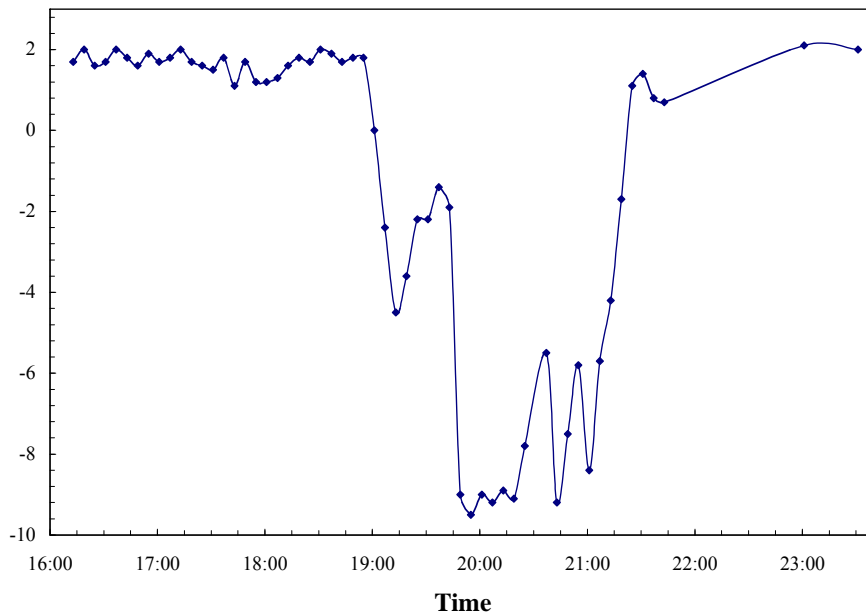
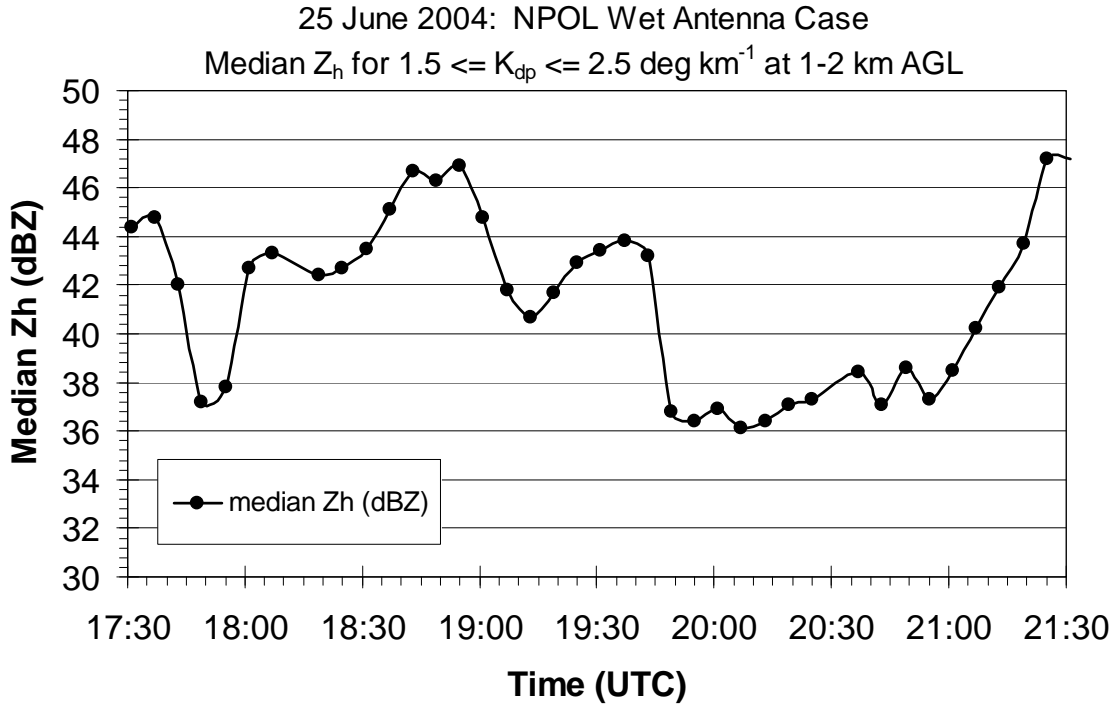


Fig. 8 Times series of reflectivity comparison between NPOL and NEXRAD. NEDRAD data was not available between 2143 and 2301 UTC.



Fig

Fig. 9. Times series of NPOL median reflectivity for samples with $1.5^\circ \leq K_{dp} \leq 2.5^\circ \text{ km}^{-1}$ between 1730 and 2130 UTC.

From a previous field experiment, e.g., the Cirrus Regional Study of Tropical Anvils and Cirrus Layers – Florida Area Cumulus Experiment (CRYSTAL-FACE), we knew that the NPOL radar suffered a serious reflectivity attenuation problem when the antenna was wet. It is our interest to use the present case study to quantify the influence of wet antenna. The time series of reflectivity differences between NPOL and NEXRAD radars (Fig. 8) showed that the NPOL was generally 1.5-2 dBZ higher than NEXRAD till 1855 UTC. After the rain started, the NPOL reflectivities began to drop. A drop of 6-6.5 dBZ appeared during 1855 to 1913 UTC. There was a recovery of about 3 dBZ during the next 24 min. The most dramatic change of NPOL data occurred between 1943 and 1949 UTC. There was a sudden reflectivity drop of 7-8 dBZ (Fig. 8). The NPOL reflectivities were about 9 dBZ lower than NEXRAD reflectivities throughout the heavy rain period.

We have also plotted the time series of median reflectivity for those samples with $1.5^\circ \leq K_{dp} \leq 2.5^\circ \text{ km}^{-1}$, which is representative of heavy rain (Fig. 9). For a dry antenna and typical DSDs in heavy rain, the median reflectivity should be approximately constant at about $45 \text{ dB} \pm 2 \text{ dB}$. Any significant ($> 2 \text{ dB}$) departure below these values is indicative of wet antenna effects in this case. Except for the early hours (1730-1800 UTC) when the median reflectivity varied quite a bit because the sample size for heavy rain was too small when the rainband was at its developing stage, the trend of the median reflectivity in Fig. 9 generally matched that of the reflectivity differences between NPOL and NEXRAD shown in Fig. 8. From Figs. 8 and 9, there are two important new points to be made regarding the effect of wet antenna on NPOL reflectivity: 1) the negative reflectivity bias is not constant during the passage of a typical rainband but varies with rain rate and hence likely degree of “wetness”

of the antenna, and 2) after the rain ended, it took about 40-50 min for the antenna to return back to its normal status.

5. Optimal Rainfall Estimation

Table 2. NPOL Rain Rate Estimation

<p>Conditions:</p> <p>a. $Z_{dr} \geq 0.5$ dB</p> <p>b. $Z_h \geq 35$ dB and $K_{dp} \geq 0.5^\circ \text{ km}^{-1}$</p>
<p>Equations:</p> <p>1. Both conditions a. and b. are satisfied: $R(K_{dp}, Z_{dr}) = 65.24 \cdot 10^{0.060 Z_{dr}} (K_{dp})^{0.995}$</p> <p>2. Only condition a. is satisfied: $R(Z_h, Z_{dr}) = 0.0015 \cdot 10^{-0.095 Z_{dr}} (Z_h)^{0.97}$</p> <p>3. Only condition b. is satisfied: $R(K_{dp}) = 40.51 \cdot (K_{dp})^{0.759}$</p> <p>4. None of condition a. or b. is satisfied: $R(Z_h) = 0.029 \cdot (Z_h)^{0.636}$</p>

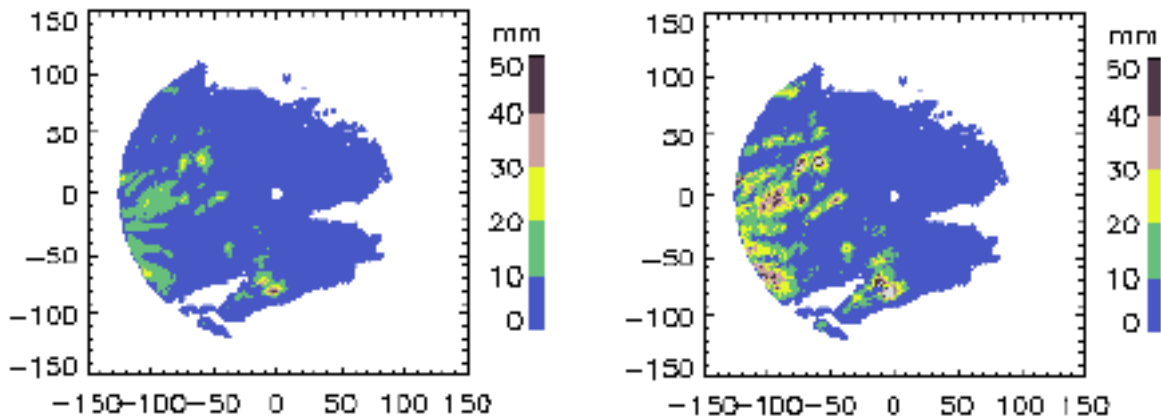


Fig.10 Total rainfall estimated from the Z-R relationship (left) and optimal polarimetric method (right) for 1613-1849 UTC, 25 June 2004.

The main objective of this project is to use the polarimetric radar measurements to improve the radar rainfall estimation. The ultimate goal is to use the improved ground-based radar

rainfall estimation to valid the rainfall estimation by satellite, e.g. TRMM and GPM. Presently, the rain rates for each radar volume were calculated using an optimization technique with the parameters Z_h , Z_{dr} , K_{dp} (Carey and Rutledge 2000). With this method, the measurement capability of each polarimetric variable is maximized. Combinations of those variables in rain rate equations (Bringi and Chandrasekar 2001) are described in Table 2. The parameters in the equations were determined based on Wallops disdrometer data analysis.

Considering that the NPOL data was contaminated by the “wet antenna” after 1850 UTC, we constructed rain map of the NPOL observational domain for the periods of 1613-1849 UTC, 25 June 2004 (Fig. 10). Compared to the traditional Z-R relationship, the optimal polarimetric method provided significantly higher rainfall amount in the heavy rain areas, especially in the strong convective region. This method was believed to give rainfall estimation close to the reality. We also calculated the frequency of each method listed in Table 1 used. The most frequently used method was $R(Z_h, Z_{dr})$, accounted for 54%. The simple Z-R relationship was used in 45% of the data. Even for such a strong convective case, the usage of K_{dp} was very rare. $R(K_{dp}, Z_{dr})$ and $R(K_{dp})$ were used 1% and 0.1%, respectively, throughout the periods.

6. Limitations and Future Work

a. The sample above is relatively small. However, many more NPOL radar volumes were investigated for error statistics and provided largely similar results (Appendix A), thus largely confirming the preliminary conclusions of Section 3 regarding the polarimetric performance of NPOL and its negative impact on rain maps. More work should be accomplished on the wet antenna issue to quantify its effects on rainfall estimation.

b. Using $20 \leq Z_h \leq 25$ dBZ is an imperfect yet expedient means of isolating “drizzle.” Ideally, you would like to have microphysically confirmed cases of drizzle in each radar volume. All cases do include wide spread echo, including heavy raining cells and widespread light rain and drizzle. Echo distribution relative to the radar and storm morphology is somewhat different on each day, which may result in slight differences in DSD, the frequency of data artifacts (e.g., side lobe contamination in high Z_h gradient regions), and the associated polarimetric response in the range of $20 \leq Z_h \leq 25$ dBZ. In the future, an effort should be made to choose more cases with nearly identical storm morphology (e.g., widespread drizzle only cases would be ideal) and verify that ranges to the target echo are similarly distributed.

c. The scanning mode varied slightly among radars (e.g., alternate vs. hybrid polarization, number of samples, rotation rate, PRF, and gate size). However, radar data in the study was collected with the typical scanning parameters utilized by each radar facility for typical polarimetric applications.

Despite the limitations of this preliminary empirical radar comparison, sensitivity tests with many other radar volumes and several other assumptions regarding the data sample suggest that the general results and associated conclusions presented herein are likely robust. Future comparative analysis will continue to address the limitations above and refine these results. An assessment of the application of NPOL data to rainfall estimation, DSD characterization, and hydrometeor identification is ongoing and will be made using both theory and detailed comparisons with rain gauge and disdrometer data.

Appendix A. NPOL Radar Polarimetric Performance during Summer-Fall 2004

Table A1. Polarimetric Radar Characteristics in “Drizzle” (20-25 dBZ) for NPOL radar.

DATE YYMMDD	Time (UTC)*	Number Gates (N)	Median Z_h	Median K_{dp}	Median ρ_{HV}	Median $\sigma(\Psi_{dp})^{**}$	AAD*** Z_{dr}
040625 [#]	2131 - 2137	4577	22.4 dBZ	0.0° km ⁻¹	0.95	7.1°	0.9 dB
040726	1818 - 1900	2244	22.3 dBZ	0.0° km ⁻¹	0.97	9.0°	0.9 dB
040728	1143 - 2318	126374	22.5 dBZ	0.0° km ⁻¹	0.94	8.5°	1.1 dB
040729	1500 - 1900	98419	22.5 dBZ	0.0° km ⁻¹	0.94	8.5°	1.1 dB
040802	1424 - 2036	170959	22.5 dBZ	0.0° km ⁻¹	0.94	9.0°	1.0 dB
040803	0030 - 2100	444262	22.5 dBZ	0.0° km ⁻¹	0.95	9.1°	1.1 dB
040812	2032 - 2326	64521	22.1 dBZ	0.0° km ⁻¹	0.95	6.5°	0.8 dB
040813	0106 - 1824	268200	22.2 dBZ	0.0° km ⁻¹	0.95	6.9°	0.8 dB
040814	2006 - 2354	158747	23.0 dBZ	0.1° km ⁻¹	0.92	7.8°	1.1 dB
040815	0036 - 0124	118186	22.8 dBZ	0.1° km ⁻¹	0.94	7.5°	1.0 dB
040830	1724 - 2224	139492	22.5 dBZ	0.0° km ⁻¹	0.94	7.8°	1.0 dB
040908	1900 - 2354	42636	22.4 dBZ	0.0° km ⁻¹	0.95	8.0°	0.9 dB
040927	1724 - 2218	32063	22.0 dBZ	0.1° km ⁻¹	0.96	7.4°	0.8 dB
040928	1442 - 2336	147955	22.4 dBZ	0.1° km ⁻¹	0.94	7.5°	1.0 dB
ALL	ALL	1814058	22.5 dBZ	0.0° km⁻¹	0.945	8.0°	1.0 dB

* Sub-periods within the time range above when the antenna was likely wet were removed from the data sample. See Table 2 below for times that were excluded from the sample for each day.

** The standard deviation of the measured differential phase was computed at each range gate from a running, centered 21-gate sample. The value shown here is the median value from all range gates in the sample.

$$*** \text{AAD } Z_{dr} = \text{Average Absolute Deviation } Z_{dr} = \sum_{i=1}^N |Z_{DR}(i) - \bar{Z}_{DR}| / N$$

Analysis from preliminary report included for comparison but not considered for “ALL” statistics.

Table A2. Time periods excluded from analysis in Table 1 (i.e., likely raining at NPOL).

Date	Excluded Time Periods (UTC)
040625 [#]	none (raining/wet antenna period already excluded by choice of volume)
040726	none
040728	1436, 1630-1736
040729	1606-1642
040802	1512, 1548-1554, 1648-1900, 1930-2000, 2018
040803	0000-0024, 0106-0242, 0430-0500, 1018-2020
040812	2138
040813	0232-0244, 0350, 0424-0500, 0530, 0554, 0618, 0636, 0700, 0724, 0742-0748, 0818-0836, 0930-1242, 1324-1330, 1518-1630
040814	2048-2236, 2300-2324
040815	none (raining period already excluded)
040830	2124
040908	1930
040927	1754, 2006-2018
040928	1524, 1542, 1618-1630, 1836-1948, 2018

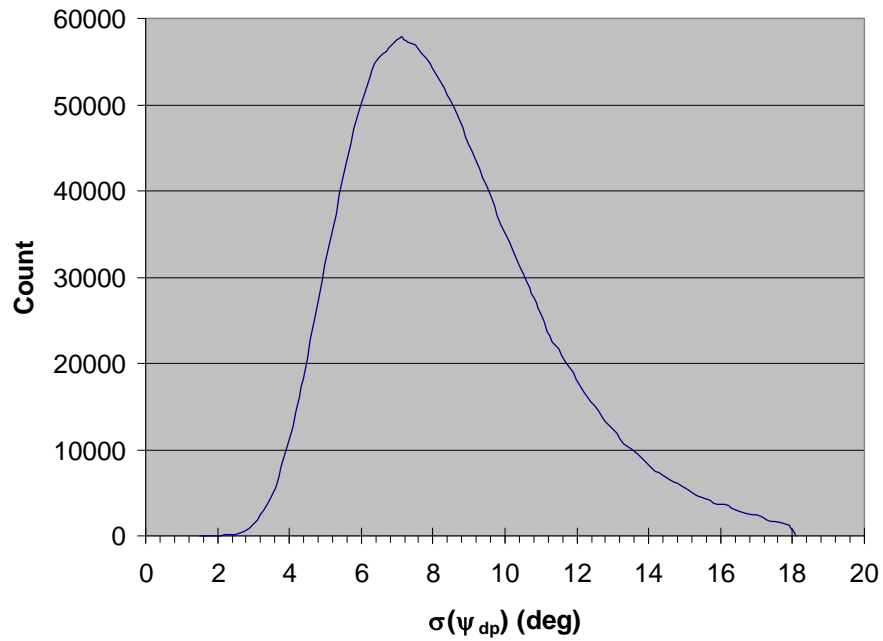


Figure A1. Frequency histogram of the standard deviation of the measured differential phase (taken over running 21 gate sample) in “drizzle” (20-25 dBZ). Bin size is 0.2° . Total sample size is 1,814,058 range gates taken from periods shown in Tables A1 and A2.

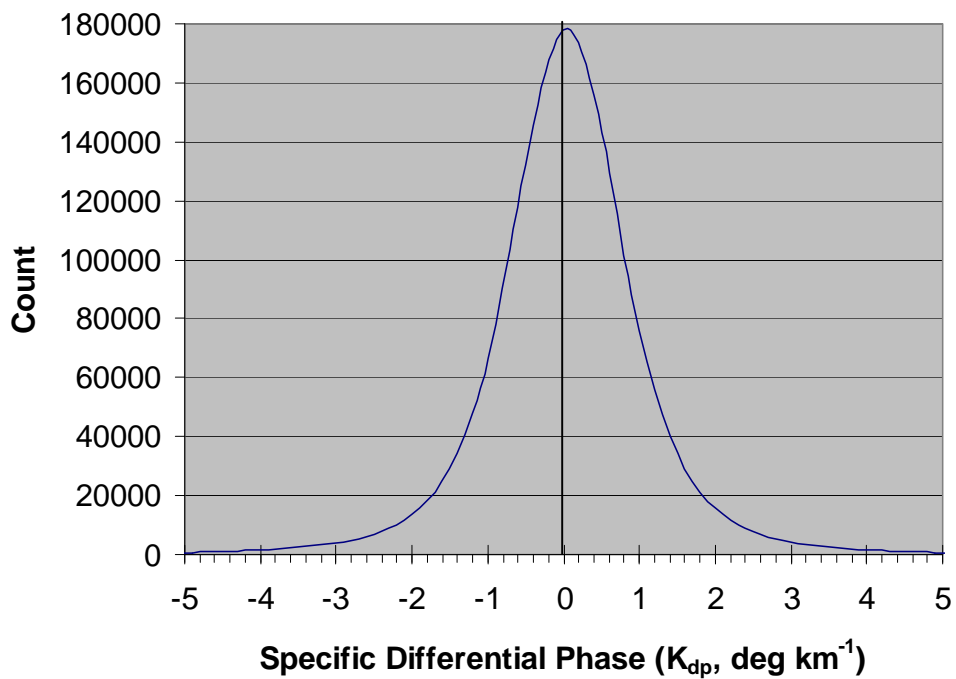


Figure A2. Same as Figure A1 except for specific differential phase. Bin size is $0.2^\circ \text{ km}^{-1}$.

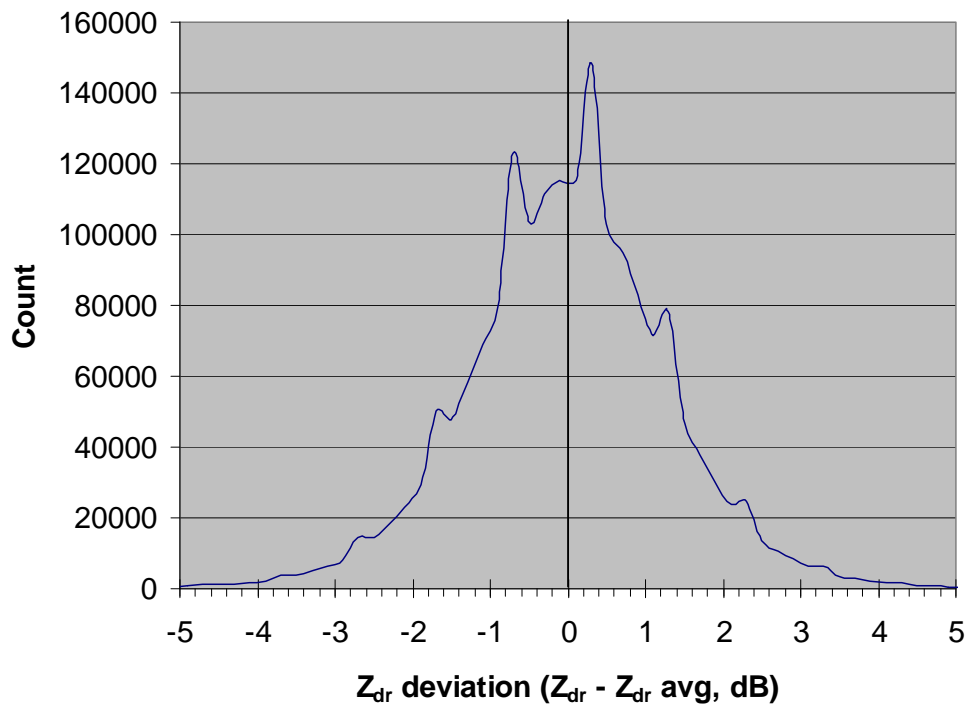


Figure A3. Same as Figure A1 except for deviation of the differential reflectivity from its mean value. Bin size is 0.2 dB.

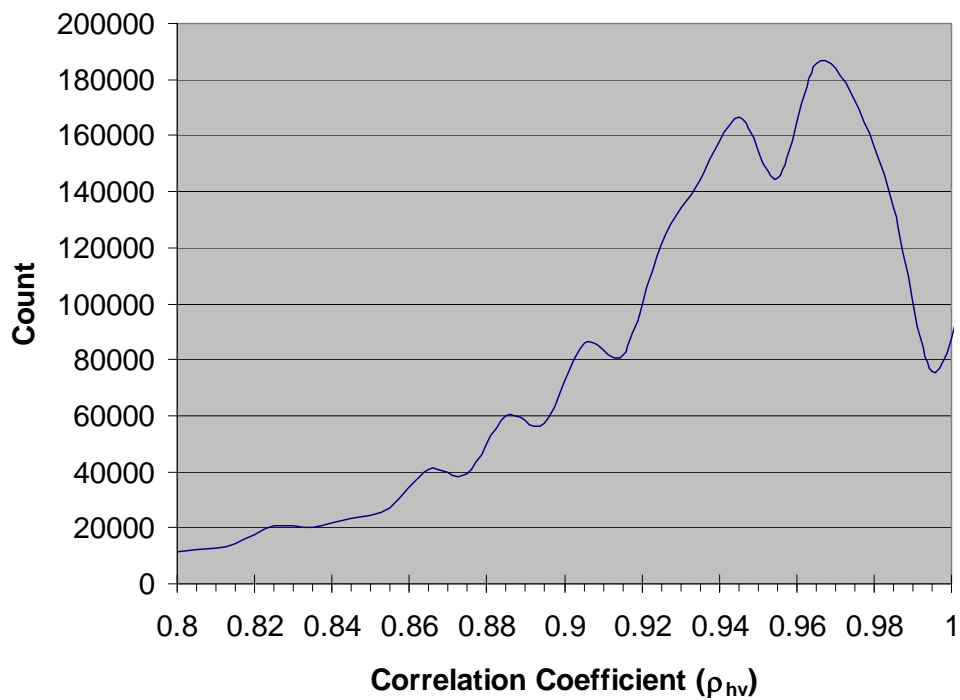


Figure A4. Same as Figure A1 except for the co-polar correlation coefficient between the hh and vv return signals. Bin size is 0.01.